Received: 22 November 2017 | Revised: 14 February 2018 | Accepted: 16 February 2018

DOI: 10.1002/chir.22852

SPECIAL ISSUE ARTICLE

WILEY

Self-assembly and chiroptical properties in supramolecular complexes of adenosine phosphates and guanidinium-bispyrene

Marie Trévisan[1] | Mathieu Fosséprè[1] | Delphine Paolantoni[2] | Jenifer Rubio-Magnieto[1] | Pascal Dumy[2] | Sébastien Ulrich[2] | Mathieu Surin[1]

[1] Laboratory for Chemistry of Novel Materials, Center of Innovation and Research in Materials and Polymers, University of Mons—UMONS, Mons, Belgium

[2] Institut des Biomolécules Max Mousseron (IBMM, UMR 5247), Université de Montpellier, CNRS, ENSCM, Montpellier, France

Correspondence

Mathieu Surin, Laboratory for Chemistry of Novel Materials, Center of Innovation and Research in Materials and Polymers, University of Mons—UMONS, 20 Place du Parc, 7000 Mons, Belgium.
Email: mathieu.surin@umons.ac.be

Sébastien Ulrich, Institut des Biomolécules Max Mousseron (IBMM, UMR 5247), Université de Montpellier, CNRS, ENSCM. Ecole Nationale Supérieure de Chimie de Montpellier, 240 Avenue du Professeur Emile Jeanbrau, 34296 Montpellier Cedex 5, France.
Email: sebastien.ulrich@enscm.fr

Funding information

ANR, Grant/Award Number: ANR-11-PDOC-002-02, ANR-10-LABX-05-01; Fonds de la Recherche Scientifique—FNRS, Grant/Award Number: F.4532.16, 1.B333.15F; COST, Grant/Award Number: CM1304; LabEx CheMISyst, Grant/Award Number: ANR-10-LABX-05-01

Abstract

Supramolecular systems that respond to the hydrolysis of adenosine phosphates (APs) are attractive for biosensing and to fabricate bioinspired self-assembled materials. Here, we report on the formation of supramolecular complexes between an achiral guanidinium derivative bearing two pyrene moieties, with each of the three adenosine phosphates: AMP, ADP, and ATP. By combining results from circular dichroism spectroscopy and molecular modeling simulations, we explore the induced chirality, the dynamics of the complexes, and the interactions at play, which altogether provide insights into the supramolecular self-assembly between APs and the guanidinium-bispyrene. Finally, we identify the chiroptical signals of interest in mixtures of the guanidinium derivative with the three APs in different proportions. This study constitutes a basis to evolve toward a chiroptical detection of the hydrolysis of APs based on organic supramolecular probes.

KEYWORDS

adenosine phosphates, ATP, circular dichroism, guanidinium, molecular dynamics, supramolecular self-assembly

[This article is part of the Special Issue: Proceedings 16th International Conference on Chiroptical Spectroscopy, Rennes France 2017. See the first articles for this special issue previously published in Volumes 30:4 and 30:5. More special articles will be found in this issue as well as in those to come.]
Marie Trévisan and Mathieu Fosséprè contributed equally to this work.
Jenifer Rubio-Magnieto's current address: Bioinspired Supramolecular Chemistry and Materials Group, Departamento de Química Inorgánica y Orgánica, Universitat Jaume I, Avda Sos Baynat s/n E-12071-Castellón, Spain.

1 | INTRODUCTION

Adenosine triphosphate (ATP) is involved in numerous biological processes, the most well known being its major role as chemical fuel for biomolecular machines operating within cells. The real-time detection of the enzymatic ATP hydrolysis has recently drawn attention, notably for achieving detection systems for sensing in situ or within cells.[1,2] This is also relevant to the fields of enzyme-responsive structures and nanomaterials that respond to ATP signaling.[3-5] Indeed, the monitoring of ATP hydrolysis is of fundamental importance to achieve bioinspired ATP-fueled dissipative self-assembled systems, such as micellar or vesicular structures, or supramolecular polymers.[1,6-11]

To follow the evolution of ATP hydrolysis in real time, mostly metal ion complexes were exploited, in which the metal ions bind ATP.[1,2,12] The complexation between these compounds (eg, with Zn^{2+} or Tb^{3+} metal centers) and ATP yielded hybrid helical supramolecular polymers or multivalent self-assembled platforms.[1,2,5,11,12] In contrast, supramolecular systems comprising metal-free organic molecules were barely explored for monitoring ATP hydrolysis, while they offer the advantages of a large conformational diversity (hence a rapid reorganization upon binding), lower toxicity, and the versatility in organic synthesis to limit the aggregation and enhance the detection sensitivity, as compared with metal-based molecules.[13]

We have recently shown that an achiral guanidinium derivative functionalized with pyrene moieties (GuaBiPy, Figure 1) is able to self-assemble along oligonucleotides (short DNA) templates in aqueous solutions, through a set of interactions between the guanidinium and the phosphodiester backbone (electrostatic interactions and H-bonds), together with π-π interactions between pyrenes of the molecular guests along the template, as observed through fluorescence signals.[14-16] Importantly, we also observed induced circular dichroism (ICD) signals (in the region where pyrenes absorb) upon interaction between the GuaBiPy (achiral) and DNA (chiral), these signals being strongly sensitive to the DNA length.[14] Given these properties, we reasoned that the GuaBiPy molecule could be exploited as a purely organic system (ie, without metal ions) to interact with various adenosine phosphates (APs), possibly yielding different supramolecular structures and chiroptical signals as a function of the number of phosphates in the AP. Indeed, circular dichroism (CD) spectroscopy has been shown to be a powerful tool to probe the induction/amplification of chirality in supramolecular systems,[17-19] especially for (oligo)nucleotide-templating systems in which the biomolecule induces a chiral conformation/assembly to the bound achiral chromophore.[1,8,11,14,20-25] Therefore, the induced chiroptical signals of GuaBiPy could be ultimately utilized to probe the enzymatic ATP hydrolysis.

In this context, we here report the chiroptical properties of supramolecular complexes of GuaBiPy with the series of APs adenosine monophosphate (AMP), adenosine diphosphate (ADP), or ATP, in aqueous solutions. The structure and the dynamics of the resulting supramolecular complexes are studied by molecular modeling simulations, which highlight the self-assembly of AP/GuaBiPy complexes through a set of possible conformations and interactions at play. Finally, we assess the chiroptical properties of multicomponent mixtures of AMP/ADP/ATP/GuaBiPy, toward a readout of the proportions of the various APs in aqueous solutions, which could be helpful to further develop detection of enzymatic hydrolysis of ATP through a chiroptical readout.

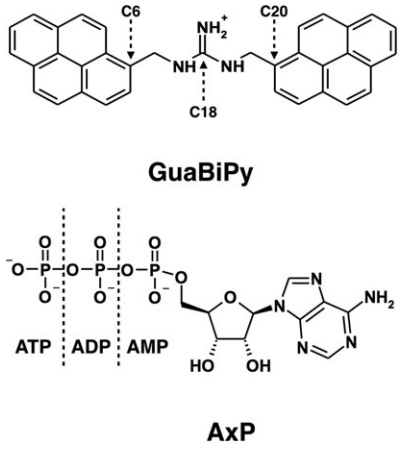

FIGURE 1 Chemical structures of GuaBiPy and adenosine phosphates (AxP: adenosine monophosphate, adenosine diphosphate, and adenosine triphosphate) under study. Three atoms (ie, C6, C18, and C20) are pointed on GuaBiPy as referred to in the text

2 | MATERIALS AND METHODS

2.1 | Materials

Adenosine triphosphate, ADP, and AMP were purchased from Sigma-Aldrich, and a stock solution of each AP (AxP) was prepared in Milli-Q water at concentration 1 mmol L^{-1}. The concentration of the aliquot of AxP in the buffer solution was verified by UV-Vis using the specific extinction coefficients (ε_0 260 nm) of AxP at 298 K, which is 15,400 L mol^{-1} cm^{-1}. Bis-*N*,*N*-(pyren-1-ylmethyl)guanidinium trifluoroacetate (GuaBiPy) was synthesized as detailed in Paolantoni et al.[14] A stock solution of GuaBiPy was freshly prepared (for each day of experiment) with 10-mmol L^{-1} molar concentration in dimethyl sulfoxide. For the titration experiments (GuaBiPy in excess), a small volume (5-10 μL) of stock

solution of GuaBiPy was diluted in 300-μL milli-Q water until the absorbance at 329 and 343 nm reached 0.7. Then, solutions of AxP and GuaBiPy (to cancel dilution effects) were added in the solution to obtain the working AxP/GuaBiPy ratios. Note that the solutions for which ATP is in excess of GuaBiPy (inverse titration) showed the presence of aggregates immediately after the addition of GuaBiPy, with no ICD signal in the absorbance range of GuaBiPy (Figure S1). The ternary and quaternary mixtures were prepared by mixing two (for ternary mixture) or three (for quaternary mixture) AxP solutions with various molar ratios between the different APs (1 mmol L^{-1} total concentration in APs); those mixtures were then added to the GuaBiPy solution (Abs [329 nm] = 0.7) to obtain a molar ratio AP mixture/GuaBiPy = 1:10.

2.2 | Methods

2.2.1 | Spectroscopy

Ultraviolet-visible absorption and CD spectra were recorded in 2-mm path length quartz cuvettes, and measurements were performed on a Chirascan™ Plus CD spectrometer (Applied Photophysics) with a bandwidth and step of 1 nm and with a time per point of 0.5 s. All experiments are performed in milli-Q water at 293 K. The experiments were performed by using a TC125 temperature controller from Quantum Northwestern running on the spectrophotometer, and the temperature within the quartz cells was determined by using a temperature probe.

2.2.2 | Molecular dynamics simulations

Molecular modeling was performed to study the dynamics of [AxP · GuaBiPy] systems at the molecular scale in an explicit water solvent. We considered one AxP molecule with a number of 4 GuaBiPy molecules as model systems to highlight the interactions at play during the self-assembly process. To build these systems, each GuaBiPy (parameterized based on an earlier study[26]) was oriented around a central AxP by using University of California, San Francisco Chimera software.[27] GuaBiPy and AxP molecules were initially separated by 15 Å, according to their geometric centers, a larger distance than the cut-off of nonbonded interactions, to avoid any bias on the recognition modes between the compounds. Figure S2 depicts the starting arrangements for the three [$AxP_1 \cdot GuaBiPy_4$] systems. Each system was then solvated within a truncated octahedral periodic box of 70 Å per side size with the TIP3P water model by using a 10 Å distance from any solute atom. An appropriate number of Cl^- counterions were added to neutralize the systems (ie, one and two Cl^- counter-ion(s) for [$ADP_1 \cdot GuaBiPy_4$] and [$AMP_1 \cdot GuaBiPy_4$], respectively). The [$ATP_1 \cdot GuaBiPy_4$], [$ADP_1 \cdot GuaBiPy_4$], and the [$AMP_1 \cdot GuaBiPy_4$] molecular systems were composed of 15,749, 15,305, and 15,344 atoms, respectively. The same molecular dynamics (MD) protocol was applied for the three [$AxP_1 \cdot GuaBiPy_4$] systems. Molecular dynamics simulations were performed with the parmbsc1 force field for the AxP molecules, one of the most recent and state-of-the-art Amber force field modifications.[28,29] Additional parameters were considered for the polyphosphate chains of ADP and ATP molecules.[30] For GuaBiPy molecules, GAFF parameters were employed with partial atomic charges calculated within AmberTools by using AM1-BCC method.[31] Electrostatic interactions were calculated via the particle mesh Ewald (PME) method with a cutoff value of 8 Å and a 2 Å as width of the nonbonded Layer. Initial minimization was done in 10,000 steps with 500 steps of steepest descent optimization followed by 9500 steps of conjugate gradient minimization with a 25 kcal mol^{-1} $Å^{-2}$ positional restraint applied to the AxP and GuaBiPy atoms. Afterward, a heating period of 1 ns was carried out in a two-step method by using the same restraint force constant on solutes. A 2 fs integration time step was used. The first step corresponds to the rise of the temperature from 100 to 300 K over 10,000 steps and then a 490,000-step equilibration stage in the NVT ensemble at the constant temperature of 300 K, controlled by a Langevin thermostat. SHAKE constraints were used to freeze bonds with hydrogen atoms. Next, the harmonic restraints were decreased to the solutes during 5 ns of MD equilibration in the NPT ensemble by using a 0.5 kcal mol^{-1} positional restraint value. During this equilibration stage, the solvent environment reached expected density values of ~1.0. The equilibration procedure was followed by 500 ns of production simulation without any positional restraints in NPT ensemble by using constant temperature at 300 K (Langevin thermostat, collision frequency of 5.0 ps^{-1}, seed for starting velocity was randomly chosen for each restart). Molecular dynamic simulations were performed within the AMBER14 software, and trajectory analysis and MD snapshots extraction were made by using CPPTRAJ.[32] A production run of 500 ns was performed for each system. The MD snapshots were saved each ns to study the formation and the conformational dynamics of the systems.

3 | RESULTS AND DISCUSSION

3.1 | Spectroscopic titrations of AP/GuaBiPy mixtures

Adenosine monophosphate, ADP, and ATP in aqueous solutions show identical UV-Vis and CD spectra

(see Figure S3); thus, one cannot distinguish between these three APs by using these techniques. In contrast, when adding each AP solution to an aqueous solution of GuaBiPy, we observed that the CD spectra of the various mixtures were quite different even at the same charge ratio, which reflect that the binding modes between AP and GuaBiPy strongly depend on the number of phosphates in APs. In particular, ICD signals in the region where the achiral GuaBiPy absorbs (300-400 nm) were shown to be very sensitive to the nature and concentration of AP in the mixture (see Figure 2), as detailed below for each AP.

3.1.1 | ATP/GuaBiPy mixtures

Figure 2a shows CD spectra of a titration of ATP by GuaBiPy. Upon increasing the ratio of GuaBiPy, we observed that the negative band at around 255 nm decreased in intensity. In the region where GuaBiPy absorbs, a weak negative ICD signal appears at molar ratio of ATP:GuaBiPy of around 1:20. For ratio 1:50 and 1:100, a very broad, positive ICD signal is observed in the 300 to 400-nm range and the diminishing of signals in the region 230 to 300 nm (where both ATP and GuaBiPy absorb).

3.1.2 | ADP/GuaBiPy mixtures

Figure 2b shows a progressive evolution of CD signals upon the titration of ADP by GuaBiPy: The signal intensities increase for all peaks until it reaches a maximum at a 1:10 molar ratio, both in the CD signals of the nucleotide region and in the ICD of GuaBiPy. In these spectra, the ICD signals are monosignate with a double peak (maxima at 362 and 344 nm at molar ratio 1:10), a well-defined signal compared with ICD signals with ATP.

3.1.3 | AMP/GuaBiPy mixtures

With AMP, one can distinguish two sets of spectra (Figure 2c): At low molar ratios (1:1 until 1:10), the ICD signals show intense bisignate (−/+) signals on a wide portion of the spectrum (negative maximum at 379 nm; positive maxima at 355 nm and 335 nm at a molar ratio 1:10). At higher molar ratios (1:20 and above), the CD signals are less intense and the ICD becomes monosignate positive. In this molar ratio range, the CD spectra resemble to the case of ADP/GuaBiPy in shape of the signal. For the sake of comparison, Figure 3 shows CD spectra of the three supramolecular complexes at a ratio of 1:10 in AxP: GuaBiPy (AxP being AMP, ADP, or ATP). This shows that, with a large excess of cationic GuaBiPy, the signals are totally different over the complete range of the spectrum. For mixtures with AMP or ADP, these signals show different ICD signatures (bisignate for AMP and monosignate for ADP) with near to a maximal intensity, whereas the mixture with ATP at this working ratio shows a zero CD signal, even in the region where the nucleotide absorbs (Figure 3).

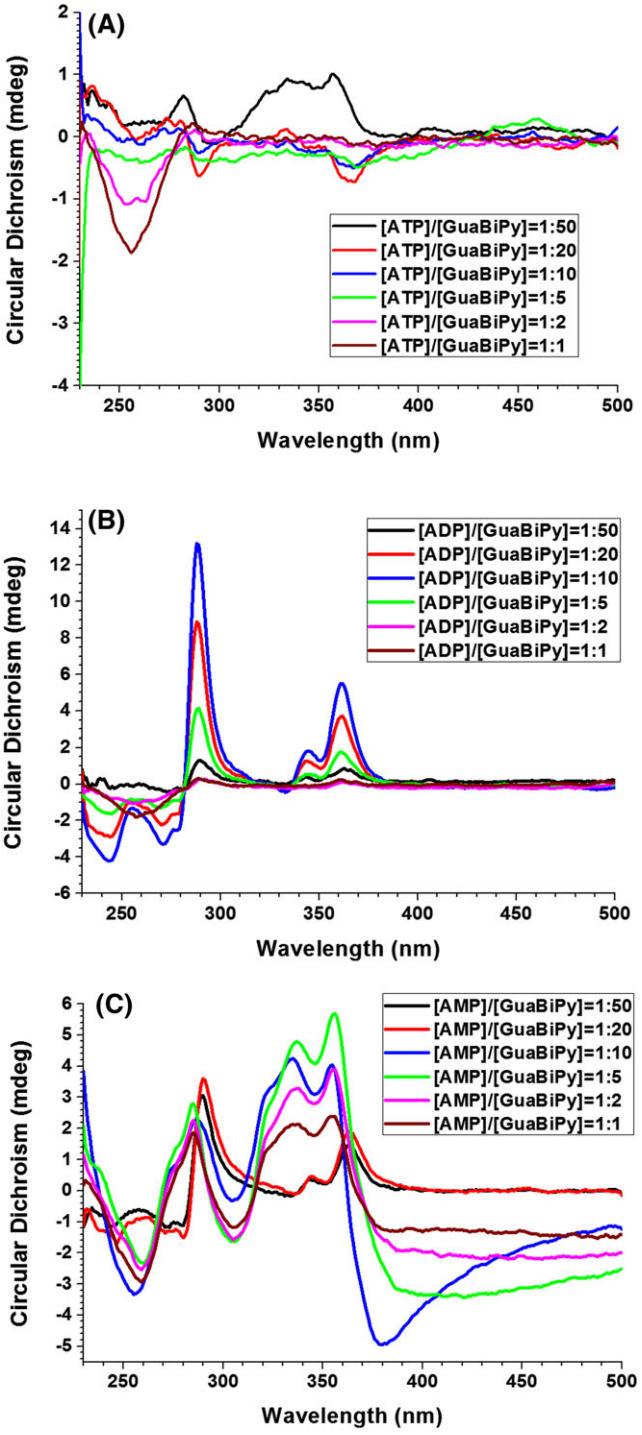

FIGURE 2 Circular dichroism spectra of mixtures of GuaBiPy with (A) adenosine triphosphate, (B) adenosine diphosphate, and adenosine monophosphate (c) at various molar ratio, in Milli-Q water at 293 K

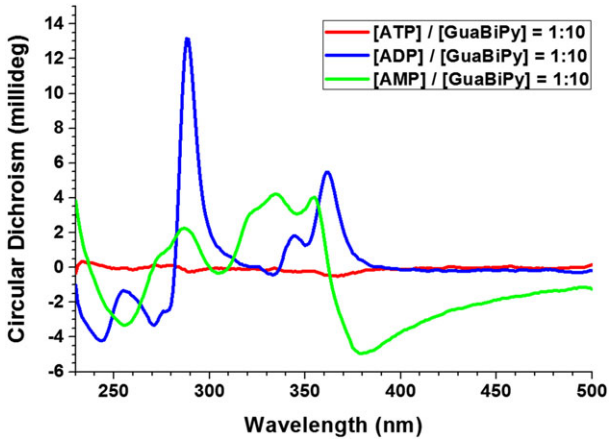

FIGURE 3 Circular dichroism spectra of mixtures of each adenosine phosphate with GuaBiPy at a molar ratio [AxP]: [GuaBiPy] = 1:10

3.2 | Molecular modeling simulations of supramolecular complexes of AP/GuaBiPy

In this section, we report the MD simulations of [AxP_1 · $GuaBiPy_4$] supramolecular complexes. Starting from noninteracting AxP/GuaBiPy molecules surrounded by an explicit water solvent model, to avoid any bias (see section 2.2), MD simulations emphasize the formation and the dynamics of the complexes on the submicrosecond timescale (500 ns) for the three [AxP · $GuaBiPy_4$]. These MD simulations provide insights into the early steps of the formation of supramolecular complexes between AxP and GuaBipy, in light with the conformational diversity and the interactions at play.

3.2.1 | Formation of [AxP_1 · $GuaBiPy_4$] complexes

[ATP_1 · $GuaBiPy_4$] system

The formation of the [ATP_1 · $GuaBiPy_4$] complex is a two-step process. As a first step, we observed the rapid formation, during the first 20 ns, of a complex between the four GuaBiPy molecules (Figure 4). The [$GuaBiPy_4$] complex is originated from π-stacking interactions between the pyrene moieties. Interestingly, the presence of an sp^3 carbon atom between the guanidinium and pyrene moieties implies that the orientations of pyrene moieties of each GuaBiPy molecule can be parallel or antiparallel (Figure 4). The self-assembly of the 4 GuaBiPy molecules presents either ″U-like″ or ″Z-like″ conformational arrangement of GuaBiPy, as depicted by the 20-ns MD snapshot (Figure 4). As a second step, the complexation between the ATP molecule and the GuaBiPys is driven by charge-assisted H-bonding between the guanidinium group and phosphate chain. The distances between the guanidinium hydrogen atom and phosphate oxygen vary between 1.8 and 2.2 Å, as observed for the structure at 40 ns (bottom left Figure 4). The complex [ATP_1 · $GuaBiPy_4$] is stable over the submicrosecond time

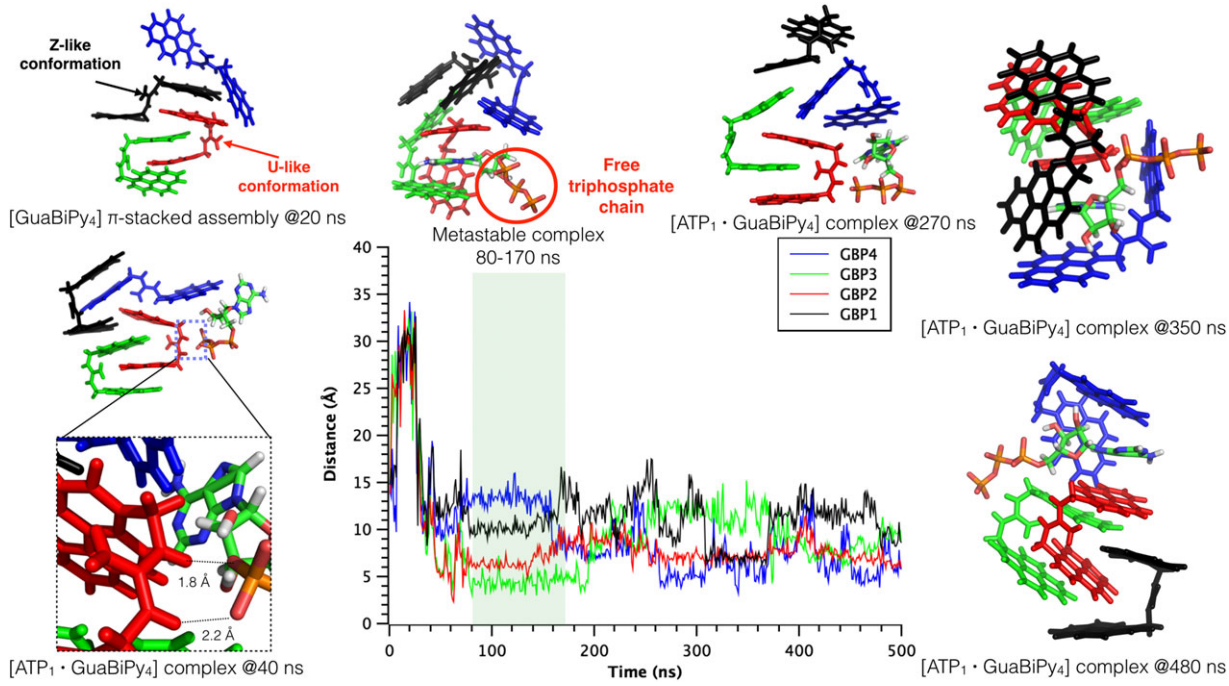

FIGURE 4 (center) Distance profiles between each GuaBiPy and adenosine triphosphate (ATP; distances between geometrical centers of molecules) along the 500-ns molecular dynamics (MD) simulation of an [ATP · $GuaBiPy_4$] system. The distances were calculated every 0.5 ns. Several snapshots are shown at various MD time, in relation with the text. A color code is used to differentiate each of the four GuaBiPy molecules

scale: No decomplexation was observed during the rest of the MD simulation, as seen in the profile of the inter-distance between each GuaBiPy and the ATP (center Figure 4), which remained below 15 Å. Interestingly, we observed a complex in which the adenine of ATP intercalates in between two pyrenes of two GuaBiPy (from 80 to 170 ns; Figure 4, top), leaving the triphosphate chain at the periphery of the complex (not interacting with guanidinium groups). A series of other binding modes between the ATP and the four GuaBiPy molecules are encountered in the MD simulations (Figure 4, right), notably complexes with either purely electrostatic interactions (complexes at 270 and 480 ns) or with purely π-stacking interactions (at 350 ns). Therefore, due to the presence of the sp^3 carbon atom as linker, the complex is quite dynamic and involves various patterns of interactions between the aromatic moieties.

[ADP_1 · $GuaBiPy_4$] system

As for the complex with ATP, the [ADP_1 · $GuaBiPy_4$] complex is rapidly formed in a two-step process with the first step being the self-assembly of 4 GuaBiPy molecules. However, the interaction between the ADP molecules and the [$GuaBiPy_4$] complex occurs via intercalation of the adenine between two pyrene moieties, as depicted with a MD snapshot at 20 ns (Figure 5). The electrostatic interactions between phosphate and guanidinium groups are significant regarding the first subsequent snapshot at 30 ns (Figure 5). In our MD simulations, the [ADP_1 · $GuaBiPy_4$] complex is less stable in comparison with the [ATP_1 · $GuaBiPy_4$], as decomplexation of the ADP molecule was observed along the 500-ns MD run. The profile of the interdistance between each GuaBiPy and the ADP shows some peaks related to the decomplexation (Figure 5), the first peak being observed at 70 ns. Nevertheless, the decomplexation is punctual as the ADP molecule is recomplexed with the [$GuaBiPy_4$] assembly as observed with the following 80-ns MD snapshot (Figure 5). A similar process was noticed; see a second peak starting at 270 ns. The MD snapshot at 280 ns, for which both a GuaBiPy and the ADP molecules do not interact with the remaining [$GuaBiPy_3$] complex, is rapidly followed by a [ADP_1 · $GuaBiPy_4$] complexation at 300 ns, stabilized by electrostactic interactions between guanidinium and phosphate groups. In this way, the transient decomplexation of the [ADP_1 · $GuaBiPy_4$] complex is alternated with electrostatic trapping that attests the preponderant role of electrostatic interactions in the self-assembly process. Similarly to the [ATP_1 · $GuaBiPy_4$] complex, the sp^3 carbon atoms of GuaBiPy lead to an important conformational dynamics, and thus, various binding modes are encountered.

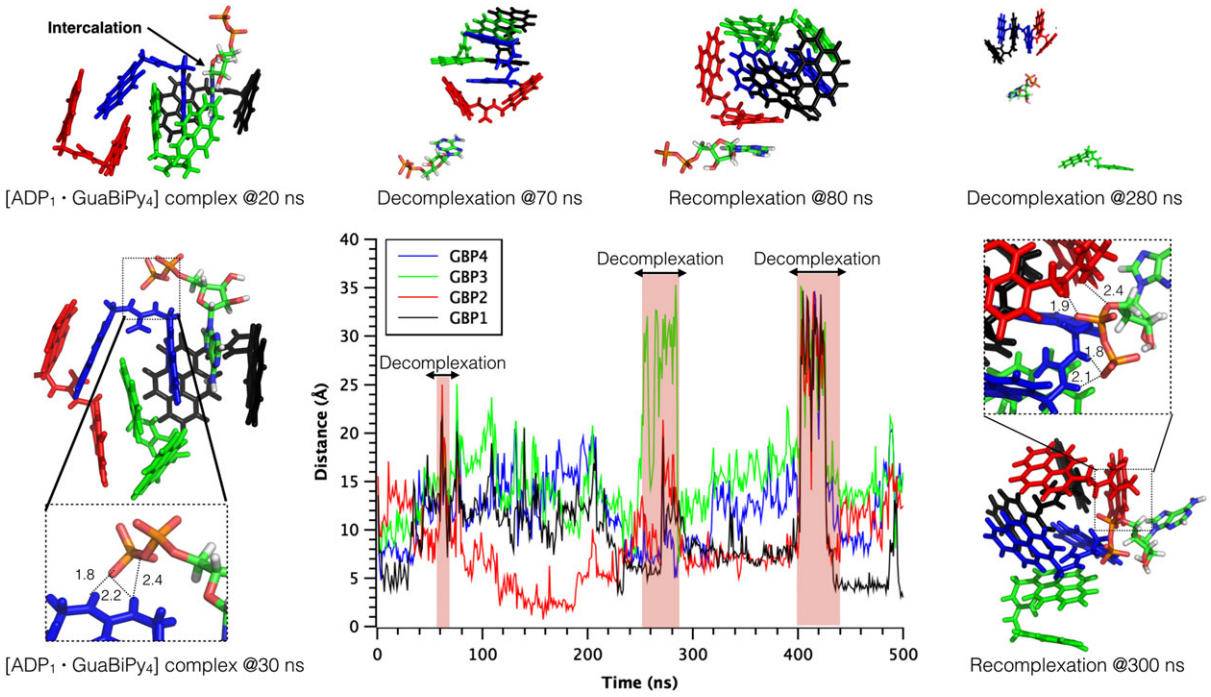

FIGURE 5 (center) Distance profiles between each GuaBiPy and adenosine diphosphate (ADP; distances between geometrical centers of molecules) along the 500-ns molecular dynamics (MD) simulation of an [ADP · $GuaBiPy_4$] system. The distances were calculated each 0.5 ns. Several snapshots are shown at various MD times, in relation with the text. A color code is used to differentiate each of the four GuaBiPy molecules

[AMP_1 · $GuaBiPy_4$] system

The formation of the [AMP_1 · $GuaBiPy_4$] complex is also rapid (within the first 40 ns) but differs from the ATP- and ADP-based complex in that there is no prior formation of a [$GuaBiPy_4$] complex observed. The formation of the complex [AMP_1 · $GuaBiPy_4$] complex is sequential with, first, the assembly between the AMP and only 2 GuaBiPy molecules throughout stacking interactions, as reported in the 20-ns snapshot (Figure 6). At 30 ns, a third GuaBiPy molecule is added to the [AMP_1 · $GuaBiPy_2$] complex, and finally, the fourth GuaBiPy molecule is stacked to the third GuaBiPy molecule to give the [AMP_1 · $GuaBiPy_4$] assembly (see Figure 6). Like the [ATP_1 · $GuaBiPy_4$] complex, the [AMP_1 · $GuaBiPy_4$] complex is stable along the 500-ns MD simulation; no decomplexation was noted. The interdistance between the AMP and each GuaBiPy molecule remains below 15 Å most of the time (Figure 6). The interdistance profile is then similar to the [ATP_1 · $GuaBiPy_4$] case with a high proximity between the AxP and each GuaBiPy molecule, resulting in a series of complexes with a tight arrangement between the subunits. After the early steps of the formation of the [AMP_1 · $GuaBiPy_4$] complex, the guanidinium-phosphate interactions are important to maintain the stability of the complex, as observed for most the snapshots of the second part of the MD simulation, ie, from 250 to 500 ns. In Figure 6, we depicted three structures: one in which there are no guanidinium-phosphate interactions between AMP and GuaBiPy molecules (250-ns snapshot) and two structures with close electrostatic interactions between the guanidinium group and the phosphate group (300 and 400-ns MD snapshots).

3.2.2 | Electrostatic interactions and phosphate accessibility

Diverse types of "electrostatic interactions," here meant to describe charge-assisted H-bonds between guanidinium and phosphate groups (at a distance of ≤2.5 Å), are encountered according to the position of the phosphate along the polyphosphate chain. The classification of the structures of the [AxP_1 · $GuaBiPy_4$] complexes is of primary importance with regard to the accessibility of the phosphate that can be influenced, or even sterically inhibited, by the complexation between GuaBiPy and APs. In this section, we focused our structural analyses on the second part MD simulations (250 to 500 ns) in light of the topology of the electrostatic interactions between AxP and GuaBiPy. We retained 26 structures for each [AxP_1 · $GuaBiPy_4$] system, ie, one each 10 ns. For the [ATP_1 · $GuaBiPy_4$] system, most structures (18 of 26) show a "free" terminal phosphate that is not trapped by electrostatic interactions with a GuaBiPy molecule. In addition, we reported in the previous section that a metastable complex with a completely "free" phosphate chain was observed in the first part of the MD simulation (0-

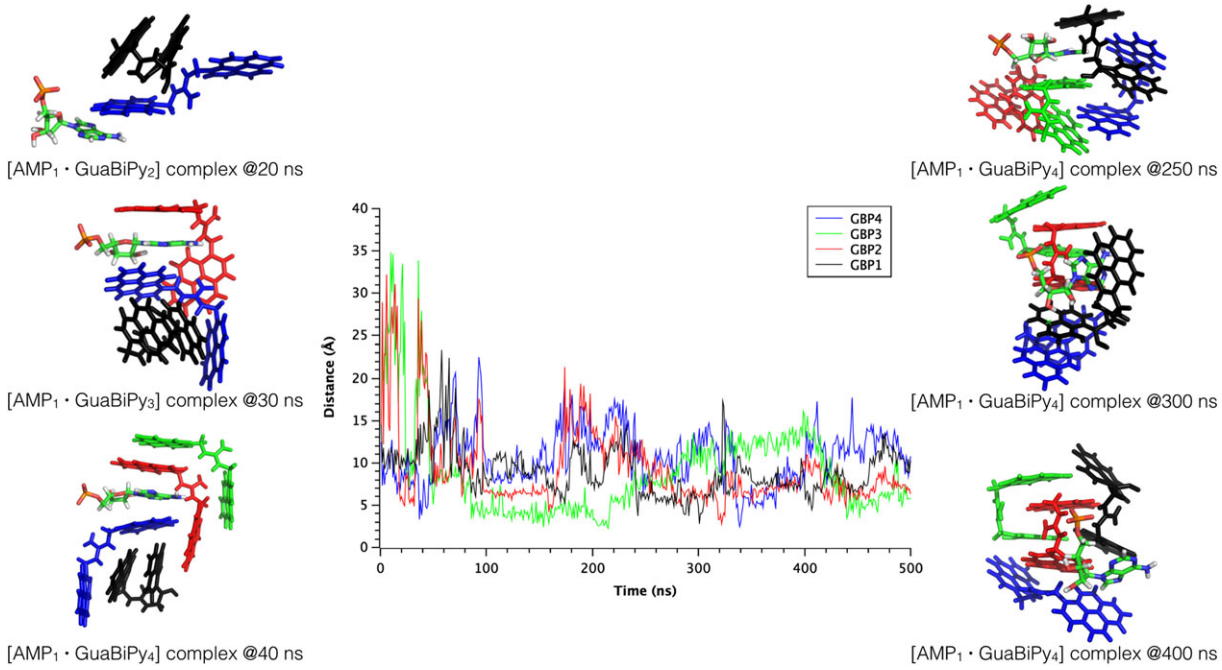

FIGURE 6 (center) Distance profiles between each GuaBiPy and adenosine monophosphate (AMP; distances between geometrical centers of molecules) along the 500-ns molecular dynamics (MD) simulation of an [AMP · $GuaBiPy_4$] system. Distances were calculated each 0.5 ns. Several snapshots are shown at various MD times, in relation with the text explanations. A color code is used to differentiate each of the four GuaBiPy molecules

250 ns) for an important existence time (80-170 ns), emphasizing the possibility of an enzyme such a phosphate to dephosphorylate the ATP even in the presence of GuaBiPy molecules in its vicinity. For the $[ADP_1 \cdot GuaBiPy_4]$ system, only 23 structures were inspected, three MD snapshots being rejected as associated to a decomplexed structure. We observed that many structures (16 of 23) are related to a terminal phosphate that is not involved in electrostatic interactions. Among the 16 structures, 8 structures are stabilized by electrostatic interactions with the nonterminal phosphate, while only stacking interactions without electrostatic interactions being encountered within the eight remaining structures. Therefore, the $[ADP_1 \cdot GuaBiPy_4]$ complexes with a free terminal phosphate are frequent in our MD simulation, leaving room around the terminal phosphate for a dephosphorylation mechanism by an enzyme. For the $[AMP_1 \cdot GuaBiPy_4]$ system, electrostatic interactions between the unique AMP phosphate and the guanidinium moiety of GuaBiPy are predominant within the structures of the complexes. The AMP phosphate is implicated in electrostatic interactions for most structures (24 of 26 structures). As a consequence, the self-assembly of ADP with four GuaBiPy molecules could block the access to the phosphate moiety and therefore inhibit of a potential enzymatic activity.

3.2.3 | Conformational flexibility and stacking interactions

The $[AxP_1 \cdot GuaBiPy_4]$ complexes are quite dynamic in view of the multiple patterns of electrostatic and stacking interactions between the GuaBiPy and the APs, leading to multiple binding modes. However, a detailed visual inspection of the complexes reveals similarities for individual GuaBiPy molecule. Whereas the presence of a sp^3 carbon atom linker between the guanidinium and the pyrenes in GuaBiPy may suggest a large panel of possible orientations, the pyrene moieties are most of the time either in a parallel (U-like conformer) or antiparallel (Z-like conformer) orientation (Figure 4). The angle C6-C18-C20 (Figure 1), which characterizes a "bending" of the pyrene-guanidinium-pyrene angle, was monitored along MD runs for all GuaBiPy in the various complexes; see Table 1. We observed Gaussian-like angle distributions with similar statistical characteristics (ie, average and standard deviations) for the three $[AxP_1 \cdot GuaBiPy_4]$ assemblies (Table 1). The average values of this angle are around 139° ± 15° for complexes with ATP and around 135° ± 16 for AMP. This particular angle originates from the geometry of the GuaBiPy molecule (in U-like or Z-like conformations) and the stacking interactions between pyrenes of adjacent GuaBiPys, which is a commonly observed throughout the MD simulations for all complexes. Therefore, the conformational diversity of GuaBiPy molecules is limited by the stacking interactions between GuaBiPy molecules, which is likely related to the defined ICD signals of GuaBiPy induced by AxPs.

3.3 | Quaternary mixtures AMP/ADP/ATP/GuaBiPy

To further assess whether the dynamic supramolecular complexes reported here could be exploited to monitor ATP hydrolysis through a chiroptical readout, we measured CD spectra at various molar ratios of APs for ternary (GuaBiPy with two different AxP) and quaternary (GuaBiPy with the three AxP) mixtures. This was achieved by changing the molar ratio between the AxP while maintaining the working ratio between the total AxP concentration and the GuaBiPy constant (with [APs]:[GuaBiPy] = 1:10); see Figure 7 (and Figure S5).

The ICD signals (ie, in the region where GuaBiPy absorbs) of ternary mixtures evolved with the composition in AxP. With pure ATP, the ICD signal is null, but by slightly increasing the proportion of AMP (without changing the ratio in ADP), an ICD signal appears whose shape is consistent with the monosignate signal of ADP hybrids but with a very low intensity, the CD signal being predominantly due to the complexes with ATP. From ratio ATP/ADP/AMP = 50:5:45 (dark blue line) to ratio ATP/ADP/AMP = 35:5:60 (light green line), a weak ICD signal

TABLE 1 Average values of the angles C6-C18-C20 for the four GuaBiPy subunit within the three $[AxP_1 \cdot GuaBiPy_4]$ self-assemblies

GBP	$[ATP_1 \cdot GuaBiPy_4]$	$[ADP_1 \cdot GuaBiPy_4]$	$[AMP_1 \cdot GuaBiPy_4]$
1	139.4 (15.7)	136.3 (14.2)	132.9 (17.6)
2	137.7 (14.3)	137.7 (16.8)	134.8 (14.8)
3	139.7 (13.1)	135.7 (19.8)	134.5 (17.0)
4	138.8 (16.0)	134.3 (14.4)	136.5 (15.0)

The corresponding standard deviations are in parentheses. ADP, adenosine diphosphate; AMP, adenosine monophosphate; ATP, adenosine triphosphate; GBP, glycerate 1,3-bisphosphate.

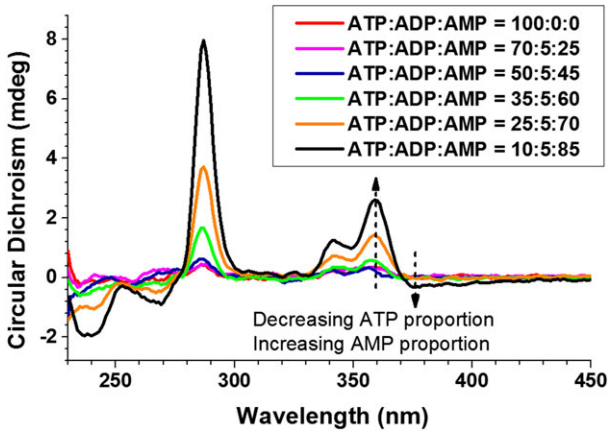

FIGURE 7 Evolution of the circular dichroism signal with the composition of a quaternary mixture GuaBiPy-ATP-ADP-AMP (at a ratio [APs]:[GuaBiPy] = 1:10)

emerges from the background noise (see zoom in Figure S5, bottom). The intensity of the signal at 365 nm further increases when the proportion in ATP decreases, while that of AMP increases, the hybrids with AMP or ADP both presenting a positive signal around this wavelength. Above a ratio ATP/ADP/AMP = 35:5:60, the ICD signal of the AMP complexes becomes prevalent, resulting in a bisignate (−/+) ICD signal (see arrows Figure 7). Remarkably, for quaternary mixtures, the ICD signals can be reproduced by using the signals from ternary mixtures. By plotting an average signal between the CD traces of two ternary mixtures, the obtained trace is almost identical as the spectrum of a quaternary mixture. For instance, by plotting an average trace between the CD spectrum of the mixture ATP/AMP = 20:80 and the CD spectrum of ADP/AMP = 10:90 (composition of the average ATP/ADP/AMP = 10:5:85, pink line in Figure 8), the obtained

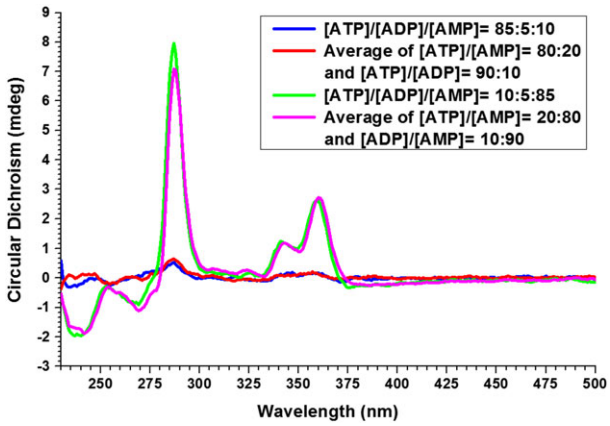

FIGURE 8 Correlation between the ternary and the quaternary mixtures with a fixed molar ratio [mixture of APs/GuaBiPy] = 1:10. The average trace between those of two ternary mixtures can be correlated to the spectrum of quaternary mixtures containing the same proportion of the different adenosine phosphates

trace is almost identical to the spectrum of the quaternary mixture at exactly ATP/ADP/AMP = 10:5:85 (green line Figure 8). This result points to the possible estimate of the composition in a mixture of AMP, ADP, and ATP, through the deconvolution of well-defined ICD signals of GuaBiPy.

4 | CONCLUSION

In this study, we have used a synthetic organic molecule, GuaBiPy, to complex APs through guanidinium-phosphate interactions. The CD spectra of aqueous mixtures show large variations depending on the type of AP and the molar ratio, in particular in the induced CD signals of GuaBiPy. The induced CD signals are different for the same molar ratio between AxP and GuaBiPy. We have shown that the change of composition in a mixture of AMP, ADP, and ATP with GuaBiPy can then be followed and deduced from the CD spectra, by correlating with the average spectra of mixtures. Besides, MD simulations reveal the differences in the dynamics of self-assembly for the various complexes and highlight the role of the conformational diversity and phosphate accessibility on the formation of the AP:GuaBiPy complexes. It is worth noticing that most conformations of complexes with ATP or ADP show a "free" terminal phosphate that is not trapped by electrostatic interactions with a GuaBiPy molecule. This is important with respect to the enzymatic activity toward APs, in the sense that the GuaBiPy molecules are likely not playing the role of an inhibitor, by leaving room for an access to the ATP triphosphate chain. Therefore, both experiments and molecular modeling indicate that guanidinium-based π-conjugated molecules could be utilized as organic chiroptical reporter for the detection of enzymatic activity, ie, hydrolysis by a phosphatase or phosphorylation by a kinase. This approach, coupled to conventional adenosine-phosphates assays, could possibly help in the analysis of the composition in APs or other nucleotide phosphates, as recently reported for supramolecular polymers and conjugated copolymers.[1,11,33] Moreover, the possibility of using guanidinium-based photoresponsive molecules with GuaBiPy in multicomponent assemblies could also be exploited,[26] for instance to modulate ATP release within dynamic supramolecular systems.

ACKNOWLEDGMENTS

Research in Mons was supported by the Fonds de la Recherche Scientifique—FNRS under the grants 1. B333.15F (CHIRNATES) and F.4532.16 (MIS-SHERPA). Research in Montpellier was supported by the ANR

(ANR-11-PDOC-002-02) and the LabEx CheMISyst (ANR-10-LABX-05-01). J.R.M., M.F., and M.S. are F.R.S.-FNRS researchers. The authors thank COST Action CM1304 (Emergence and Evolution of Complex Chemical Systems) for the support of the collaboration.

ORCID

Pascal Dumy http://orcid.org/0000-0002-7660-763X
Sébastien Ulrich http://orcid.org/0000-0002-6080-3345
Mathieu Surin http://orcid.org/0000-0001-8950-3437

REFERENCES

1. Kumar M, Brocorens P, Tonnelé C, Beljonne D, Surin M, George SJ. A dynamic supramolecular polymer with stimuli-responsive handedness for in situ probing of enzymatic ATP hydrolysis. *Nat Commun*. 2014;5:5793.
2. Jung SH, Kim KY, Lee JH, et al. Self-assembled Tb^{3+} complex probe for quantitative analysis of ATP during its enzymatic hydrolysis via time-resolved luminescence in vitro and in vivo. *ACS Appl Mater Interfaces*. 2017;9(1):722-729.
3. Zelzer M, Todd SJ, Hirst AR, McDonal TO, Ulijn RV. Enzyme responsive materials: design strategies and future developments. *Biomater Sci*. 2013;1(1):11-39.
4. Biswas S, Kinbara K, Niwa T, et al. Biomolecular robotics for chemomechanically driven guest delivery fuelled by intracellular ATP. *Nat Chem*. 2013;5(7):613-620.
5. Pezzato C, Prins LJ. Transient signal generation in a self-assembled nanosystem fueled by ATP. *Nat Commun*. 2015;6(1):7790.
6. Wang C, Chen Q, Wang Z, Zhang X. An enzyme-responsive polymeric superamphiphile. *Angew Chem Int Ed Engl*. 2010;49(46):8612-8615.
7. Hao X, Sang W, Hu J, Yan Q. Pulsating polymer micelles via ATP-fueled dissipative self-assembly. *ACS Macro Lett*. 2017;6(10):1151-1155.
8. Surin M. From nucleobase to DNA templates for precision supramolecular assemblies and synthetic polymers. *Polym Chem*. 2016;7(25):4137-4150.
9. Sorrenti A, Leira-Iglesias J, Sato A, Hermans TM. Non-equilibrium steady states in supramolecular polymerization. *Nat Commun*. 2017;8:15899.
10. Maiti S, Fortunati I, Ferrante C, Scrimin P, Prins LJ. Dissipative self-assembly of vesicular nanoreactors. *Nat Chem*. 2016;8(7):725-731.
11. Dhiman S, Jain A, George SJ. Transient helicity: fuel-driven temporal control over conformational switching in a supramolecular polymer. *Angew Chem Int Ed Engl*. 2017;56(5):1329-1333.
12. Kumar M, Jonnalagadda N, George SJ. Molecular recognition driven self-assembly and chiral induction in naphthalene diimide amphiphiles. *Chem Commun*. 2012;48(89):10,948-10,950.
13. Maity D, Li M, Ehlers M, Schmuck C. A metal-free fluorescence turn-on molecular probe for detection of nucleoside triphosphates. *Chem Commun*. 2016;53(1):208-211.
14. Paolantoni D, Rubio-Magnieto J, Cantel S, et al. Probing the importance of pi-stacking interactions in DNA-templated self-assembly of bisfunctionalized guanidinium compounds. *Chem Commun*. 2014;50(91):14,257-14,260.
15. Bouillon C, Paolantoni D, Rote JC, et al. Degradable hybrid materials based on cationic acylhydrazone dynamic covalent polymers promote DNA complexation through multivalent interactions. *Chem A Eur J*. 2014;20(45):14,705-14,714.
16. Paolantoni D, Cantel S, Dumy P, Ulrich S. A dynamic combinatorial approach for identifying side groups that stabilize DNA-templated supramolecular self-assemblies. *Int J Mol Sci*. 2015;16(2):3609-3625.
17. Berova N, Polavarapu PL, Nakanishi K, Woody RW (Eds). *Comprehensive Chiroptical Spectroscopy. Applications in Stereochemical Analysis of Synthetic Compounds, Natural Products, and Biomolecules*. Wiley: United States of America; 2012.
18. Palmans AR, Meijer EW. Amplification of chirality in dynamic supramolecular aggregates. *Angew Chem Int Ed Engl*. 2007;46(47):8948-8968.
19. Pescitelli G, Di Bari L, Berova N. Application of electronic circular dichroism in the study of supramolecular systems. *Chem Soc Rev*. 2014;43(15):5211-5233.
20. Surin M, Janssen PGA, Lazzaroni R, Leclère P, Meijer EW, Schenning APHJ. Supramolecular organization of ssDNA templated π-conjugated oligomers via hydrogen-bonding. *Adv Mater*. 2009;21(10-11):1126-1130.
21. Sargsyan G, Schatz AA, Kubelka J, Balaz M. Formation and helicity control of ssDNA templated porphyrin nanoassemblies. *Chem Commun*. 2013;49(10):1020-1022.
22. Rubio-Magnieto J, Thomas A, Richeter S, et al. Chirality in DNA-pi-conjugated polymer supramolecular structures: insights into the self-assembly. *Chem Commun*. 2013;49(48):5483-5485.
23. Qiu H, Gilroy JB, Manners I. DNA-induced chirality in water-soluble poly(cobaltoceniumethylene). *Chem Commun*. 2013;49(1):42-44.
24. Rubio-Magnieto J, Kumar M, Brocorens P, et al. Chiral supramolecular organization and cooperativity in DNA-templated assemblies of Zn^{II}-chromophore complexes. *Chem Commun*. 2016;52(96):13,873-13,876.
25. Leira-Iglesias J, Sorrenti A, Sato A, Dunne PA, Hermans TM. Supramolecular pathway selection of perylenediimides mediated by chemical fuels. *Chem Commun*. 2016;52(58):9009-9012.
26. Rubio-Magnieto J, Phan TA, Fossepré M, et al. Photomodulation of DNA-templated supramolecular assemblies. *Chem A Eur J*. 2018;24(3):706-714.
27. Pettersen EF, Goddard TD, Huang CC, et al. UCSF chimera—a visualization system for exploratory research and analysis. *J Comput Chem*. 2004;25(13):1605-1612.
28. Ivani I, Dans PD, Noy A, et al. Parmbsc1: a refined force field for DNA simulations. *Nat Methods*. 2016;13(1):55-58.
29. Galindo-Murillo R, Robertson JC, Zgarbova M, et al. Assessing the current state of Amber force field modifications for DNA. *J Chem Theory Comput*. 2016;12(8):4114-4127.

30. Meagher KL, Redman LT, Carlson HA. Development of polyphosphate parameters for use with the AMBER force field. *J Comput Chem*. 2003;24(9):1016-1025.
31. Jakalian A, Jack DB, Bayly CI. Fast, efficient generation of high-quality atomic charges. AM1-BCC model: II. Parameterization and validation. *J Comput Chem*. 2002;23(16):1623-1641.
32. Roe DR, Cheatham TE 3rd. PTRAJ and CPPTRAJ: software for processing and analysis of molecular dynamics trajectory data. *J Chem Theory Comput*. 2013;9(7):3084-3095.
33. Willis-Fox N, Gutacker A, Browne MP, et al. Selective recognition of biologically important anions using a diblock polyfluorene–polythiophene conjugated polyelectrolyte. *Polym Chem*. 2017;8(46):7151-7159.

SUPPORTING INFORMATION

Additional Supporting Information may be found online in the supporting information tab for this article.

How to cite this article: Trévisan M, Fossépré M, Paolantoni D, et al. Self-assembly and chiroptical properties in supramolecular complexes of adenosine phosphates and guanidinium-bispyrene. *Chirality*. 2018;30:719–729. https://doi.org/10.1002/chir.22852